

Finite Element Solution for Thermal Analysis of NiTiNOL- 60 Ball Bearing



Karni Venkatesh

M.Tech (Thermal Engineering) Student,
Department of Mechanical Engineering,
Nadimpalli Satyanarayana Raju Institute of
Technology, Visakhapatnam.



Kona Ram Prasad

Assistant Professor,
Department of Mechanical Engineering,
Nadimpalli Satyanarayana Raju Institute of
Technology, Visakhapatnam.

ABSTRACT:

Objective: To analyze the heat transfer in a NiTiNOL-60 ball bearing and to study the heat dissipation, temperature profile, deformation and thermal stresses occurring in a bearing as a function of rotational speed.

Methods/Statistical Analysis:

The Finite Element Method (FEM) was used to analyze the heat flow and other parameters in a bearing. Modeling of the system was done using SOLIDWORKS. The analysis was done to study the heat dissipation in the bearing. The model was imported in ANSYS by giving all the parameters. The temperature profile in the bearing was obtained by changing the properties. Structural analysis was performed and the deformation of the bearing at various points were calculated.

Findings:

It was observed that the temperature of the bearing increases with increase in the heat generation. The effects of temperature for different bearing speeds have been studied and it has been found that the rotational speeds have predominant effect on the temperature. The temperature of the bearing increases with the increase in speed. The maximum temperature is a function of heat generation.

With the increase of the rotational speed the displacement increases which causes deformation and stresses. The rotational speed also has more effect on the stiffness.

Application/Improvements:

Bearing is used to support the shaft. As an improvement the vibration characteristics can be analyzed and simulated.

Introduction:

Hard, Corrosion-Proof Nickel Titanium Material for Use in Mechanical Components Shock-resistant material eliminates corrosion and polishes to a smooth surface finish NASA's Glenn Research Center has developed a new method for producing a shock- and corrosion-proof superelastic intermetallic material — NiTiNOL 60 (60NiTi) — for use in ball bearings and other mechanical components. These superelastic materials can withstand tremendous loads and stresses without permanent deformation or denting. At the same time, the nickel-titanium alloy is immune to corrosion and rust, unlike mechanical components made from iron or steel. In addition, the material does not chemically degrade or break down lubricants, a common problem with existing bearing materials. This material is best suited for oil lubricated rolling and sliding contact applications requiring superior and intrinsic corrosion resistance, electrical conductivity,

and non-magnetic properties. The goal was to develop high-temperature, nonmagnetic alloys for missile cone applications. The research identified two compositions: NiTiNOL 55 (55Ni-45Ti) And NiTiNOL 60 (60Ni-40Ti), In weight percent. Because and NiTiNOL 60 was difficult to cast and hot work with NiTiNOL 60 was suspended. Puris developed patent-pending processing methods and chemistry control around the base NiTiNOL alloy to create SM-100 – the only commercially available variant of NiTiNOL 60.

2. Materials and Methods:

Based on the literature review, the design and process parameters were selected. The steady state thermal solution was obtained. The static structural solutions were obtained. Figure 2 shows the flow chart for thermal and structural solutions.



Figure 2. Flow chart for thermal and structural solution.

2.1 Experimental Procedure:

The model includes all the heat sources and thermal expansion in the system. Friction causes an increase in temperature of the bearing. If the heat generated is not removed the bearing may fail. To analyze the heat flow, a ball bearing has been modeled and analyzed using the finite element technique. The temperature is a function of heat dissipation and the speed. The design model was created in SOLIDWORKS and was imported to ANSYS by giving the parameters and the steady state thermal analysis was done by giving the required conditions. The deformation of the bearing at various points were calculated.

NiTiNOL -60 (2215Ekn9) life CALCULATE:

Basic Rating Life and SKF Rating Life An SKF Self – Aligning ball Bearing – 2215EKN9 is to Operate at 1000 R/Min under a constant radial Load $F_r = 15\text{KN}$. Oil Lubrication is to be used, the oil has an actual kinematic viscosity $(V) = 250 \text{ MM}^2 / \text{s}$ at normal

operating Temperature. The desired reliability is 90% and it is assumed that the operating conditions are very clean.

a). The basic rating life 90% reliability is

$$L_{10} = (c/p)^3$$

From the product table for bearing 2215EKN9, $C = 58.5 \text{ KN}$ since the load is purely radial, $P = F_r = 15 \text{ kN}$ (Equivalent dynamics bearing load) .

* In million revolutions

$$L_{10} = (58.5/15)^3 = 59.3$$

* Or in operating hours

$$L_{10h} = (10^6/60 \times n) \times L_{10} = (1000000/60000) \times 59.3 = 988.3$$

Table 1. Life adjustment factor a_1

S.no.	Reliability(%)	Failure Probability (η)	SKF rating life (L_{10m})	Factor (a_1)
1.	90	10	L_{10m}	1
2.	95	5	L_{5m}	0.64
3.	96	4	L_{4m}	0.55
4.	97	3	L_{3m}	0.47
5.	98	2	L_{2m}	0.37
6.	99	1	L_{1m}	0.25

b). The SKF rating life for 90% reliability is

$$L_{10m} = a_1 a_{skf} L_{10}$$

As a reliability of 90% is required, the L_{10m} life is to be calculated and $a_1 = 1$ (table 1) from the product table for bearing 2215EKN9,

$$D_m = 0.5[d+D] = 0.5[75+130] = 102.5$$

The Rated oil viscosity at operating temperature for a speed of 1000 r/min,

$$V_1 = 11.5 \text{ mm}^2/\text{s}$$

$$K = v/v = 250/11.5 = 21.73$$

TABLE:2 Guideline values for factor η_c for different level of contamination

Conditions	Factor η_c for bearings with diameter $dm < 100$ $dm \geq 100$ mm
Extreme cleanliness Particle size of the order of the lubricant film thickness Laboratory conditions	1 1
High cleanliness Oil filtered through an extremely fine filter Typical conditions: sealed bearings that are greased for life	0,8 ... 0,6 0,9 ... 0,8
Normal cleanliness Oil filtered through a fine filter Typical conditions: shielded bearings that are greased for life	0,6 ... 0,5 0,8 ... 0,6
Slight contamination Typical conditions: bearings without integral seals, coarse filtering, wear particles and slight ingress of contaminants	0,5 ... 0,3 0,6 ... 0,4
Typical contamination Typical conditions: bearings without integral seals, coarse filtering, wear particles, and ingress from surroundings	0,3 ... 0,1 0,4 ... 0,2

From the Product table $p_u = 1.1K.N$ and $P_w/p = 1.1/15$ 0.073. As the conditions are very clean, $N_c = 0.85$ (table 2) and $N_c (P_w/P) = 0.85 (0.073)$ With $K = 21.73$ and using the S K F Explorer Scale in Table 2, the value of $a_{SKF} = 2.15$ is obtained. Then according to the SKF rating life Equation, in million revolutions

$$L_{10m} = 1 \times 2.15 \times 59.3$$

$$= 127.4$$

Or in operating hours using,

$$L_{10MH} = (10^6/60n) \times L_{10m}$$

$$L_{10MH} = (1000000/60000) \times 127.4$$

$$= 2123.3$$

Same as calculated 1100,1200,1300,1400,1500 .

TABLE: 3 Bearing Life Calculate for 90% Reliability

S. No	Parameters	1000	1100	1200	1300	1400	1500
1	Basic Rating Life in Million Resolutions	59.3	59.3	59.3	59.3	59.3	59.3
2	Basic Rating in Hours	988.3	898.4	823.96	760.2	705.9	658.8
3	SKF Rating Life in million resolution	127.4	127.4	127.4	127.4	127.4	127.4
4	Basic Rating life in Hours	2123.3	1930.3	1769.4	1633.3	1516.6	1415.4

2.1.2 Heat Generation in the Bearing

The major source of heat generation is the machining process and the friction between the balls and the races. The major portion of the heat is taken away by the coolant and the chips. In ball bearings heat is generated by three sources. First is the load related heat generation, second source is the viscous shear of lubricants between the solid bodies, known as viscous heat dissipation. The third source of heat is known as spin related heat generation. Considering this, analytical formulation for heat generation in a bearing was developed. The heat generated in a bearing is given as

$$H_f = 1 \times 10^{-4} \cdot n \cdot M \text{ -----(3)}$$

where, H_f is the heat generation due to friction in Watts, n is the rotational speed (rpm), M is the total frictional torque (N mm). Rotational speeds of 1000 ,1100, 1200, 1300,1400,1500, were taken and the total frictional torque as 100 N-mm. The internal heat generation can be calculated by using the formula, Internal Heat Generation = H_f / V . The volume of the Ball bearing was calculated as 2095mm^3 . The values were tabulated and the internal heat generation was calculate The internal heat generation for different speeds is shown in Table:4

TABLE :4 Internal Heat Generation for Different Speed

S. No	Speed (RPM)	Heat Generation (W)	Volume of Bearings MM^3	Heat Generated $(\text{NXMX}10^{-4})$	Heat Generation Unit Volume
1	1000	280 N-MM	191647	28	1.461X10-4
2	1100	286 N-MM	191647	31.46	1.619X10-4
3	1200	292 N-MM	191647	35.04	1.828X10-4
4	1300	298 N-MM	191647	37.96	1.980X10-4
5	1400	304 N-MM	191647	42.56	2.220X10-4
6	1500	310 N-MM	191647	46.5	2.42X10-4

2.1.3 Modeling in SOLIDWORKS:

The bearing consists of Nitinol 60 (2215EKTN9) balls of Volume 2095mm^3 . The outer and inner diameter are $D = 130$ mm, $d = 75$ mm respectively, $B = 15.8 \text{mm}$, $a_0 = 100^0$ and $Z = 34$ balls.

The bearing operates under dynamic load rating of $C=58.5\text{kN}$ and static load rating of $C_0 = 15 \text{ kN}$ and at a rotational speed of 1000-1500rpm.

2.1.4 Simulation:

The model made in SOLIDWORKS was imported in ANSYS. The node has three degrees of freedom; translation in the x, y, and z directions. The simulation was performed. The solid model was imported in ANSYS workbench. The steady state thermal analysis containing Engineering Data, Geometry, and Model was performed and the solution was obtained. The properties of ceramic are given as follows. Density = 6.7g/cc coefficient of thermal expansion = $12.4 \times 10^{-6} / ^\circ\text{C}$, Young's modulus = 320E9 Pa , Poisson's ratio = 0.27 . The meshing of the model was then done. The meshing of the model was then done. Figure 3 shows the imported data in ANSYS and Figure 4 shows the meshing of the assembly.

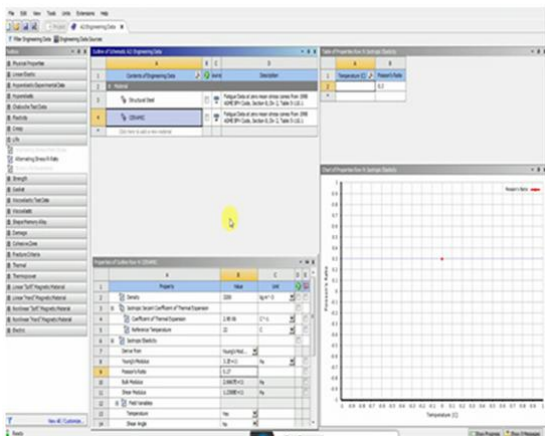


Figure 3. Importing the data in ANSYS.

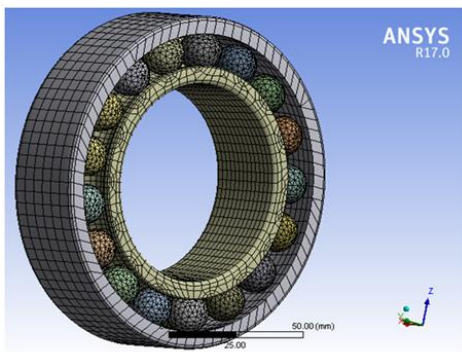


Figure 4. Meshing of the assembly

Table:5 Simulation Results

S. No	Rotational Speed (RPM)	Temperature (K)		Total Heat Flux (W/mm ²)		Total Deformation (mm)		Equivalent Stress (H bar)		Equivalent Elastic Strain (mm/mm)	
		Inner Ring	Outer Ring	Inner Ring	Outer Ring	Inner Ring	Outer Ring	Inner Ring	Outer Ring	Inner Ring	Outer Ring
1	1000	415	412	0.019	0.0022	0.040	0.031	77.84	9.46	0.003	0.0005
2	1100	436	433	0.023	0.0026	0.033	0.030	26.64	3.23	0.004	0.0007
3	1200	454	449	0.025	0.0031	0.038	0.003	33.21	4.53	0.005	0.0008
4	1300	470	465	0.031	0.0035	0.042	0.001	36.76	5.01	0.006	0.0016
5	1400	488	482	0.034	0.0038	0.046	0.015	45.30	5.50	0.007	0.0014
6	1500	507	502	0.035	0.0039	0.058	0.045	98.3	13.44	0.010	0.0015

3. Results and Discussion:

The simulation gave the required parameters which are temperature, total heat flux, total deformation, equivalent stress and equivalent elastic strain at various rotational speeds from 1000-1500 rpm. Figures 5-9 Indicate the temperature profile, heat flux, total deformation, equivalent stress and equivalent strain respectively at 1000 rpm. Figures 10-14 temperature profile, heat flux, total deformation, equivalent stress and equivalent strain respectively at 1500 rpm. The temperature, total heat flux, total deformation, equivalent stress and equivalent elastic strain values were taken from the simulated models with respect to rotational speed and were tabulated for obtaining the heat generation rate in the ball bearing.

The heat generation was calculated. The simulation results are shown in Table 5. Figure 15 shows the rotational speed (rpm) vs. Temperature plot for various range of speeds. Figure 16 represents the rotational speed (rpm) vs. total heat flux (W/mm^2) plot for different speeds. Figures 17 and 18 shows the plot of rotational speed (rpm) vs. equivalent stress (MPa) and equivalent strain. Figure 19 indicates the rotational speed (rpm) vs. total deformation (mm) plot, respectively.

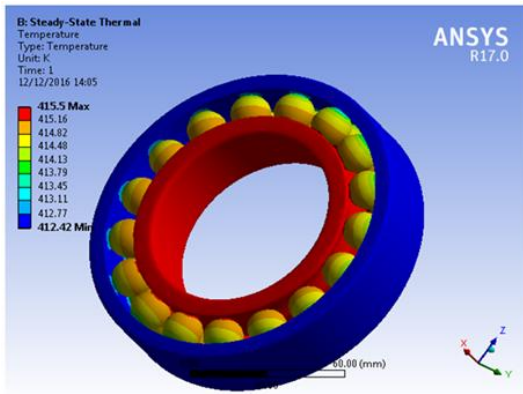


Figure 5. Temperature distribution(1000rpm).

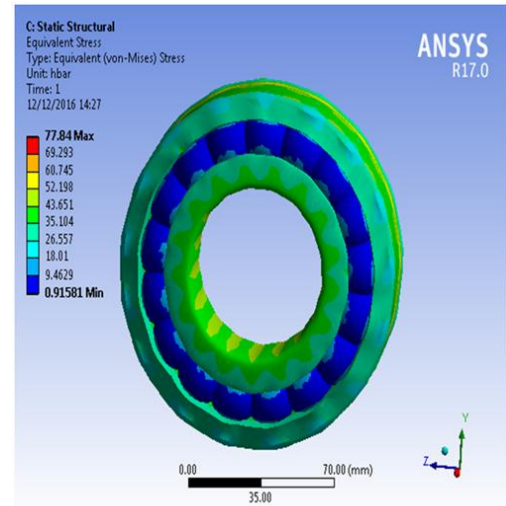


Figure 8. Equivalent stress (1000rpm).

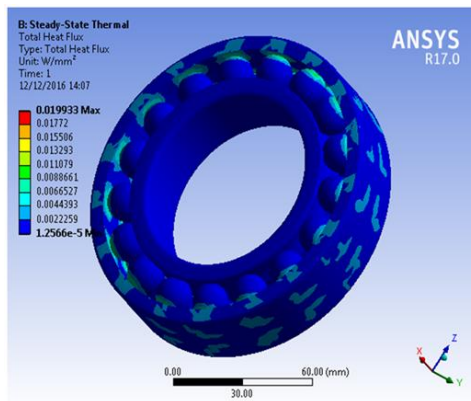


Figure 6. Total heat flux(1000rpm).

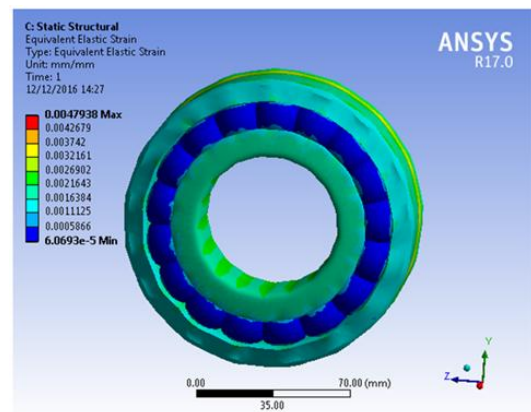


Figure 9. Equivalent strain(1000rpm).

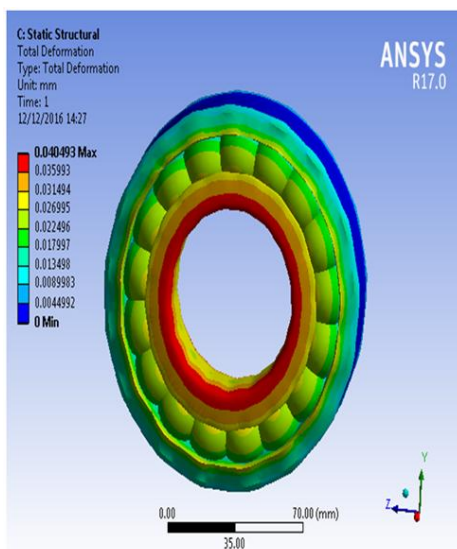


Figure 7. Total deformation (1000rpm).

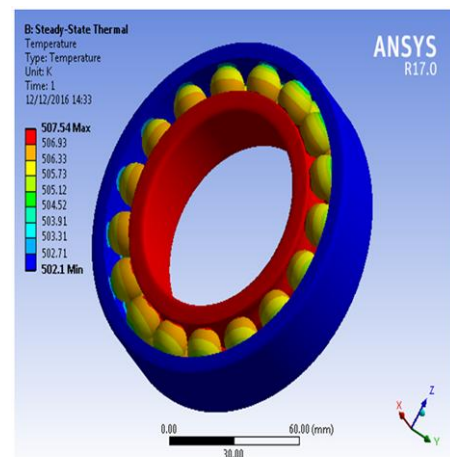


Figure 10. Temperature distribution(1500rpm)

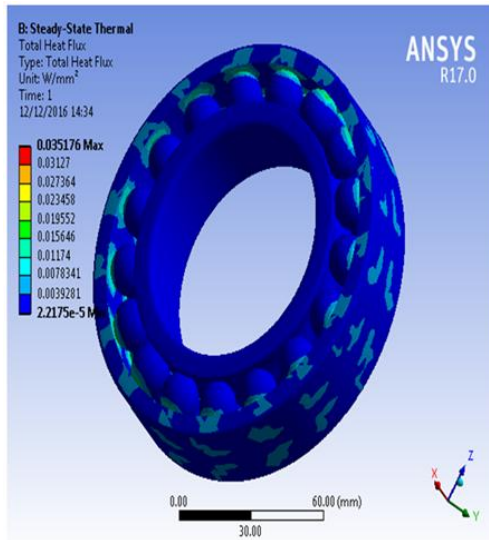


Figure 11 .Total heat flux(1500rpm).

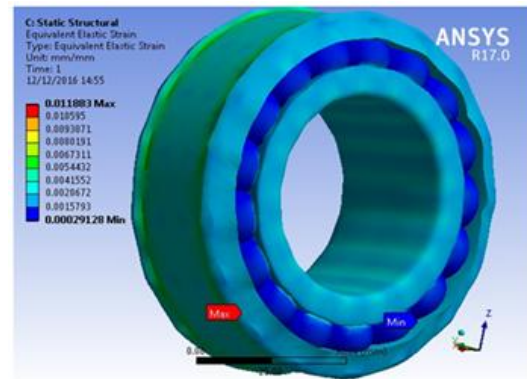


Figure 14 .Equivalent strain (1500rpm).

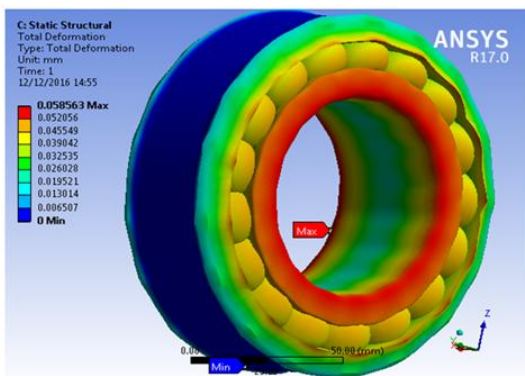


Figure 12 .Total deformation(1500rpm).

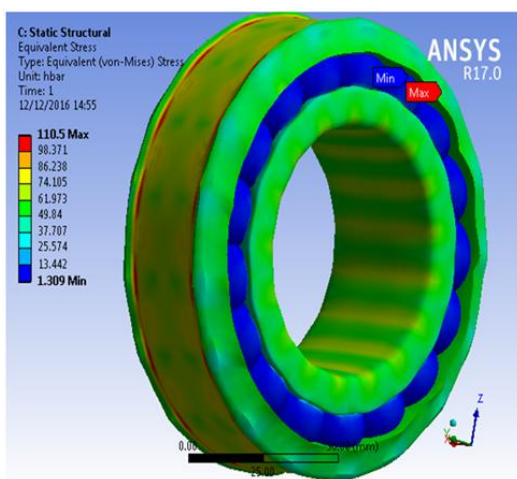


Figure 13.Equivalent stress (1500rpm).

In the numerical analysis temperature distribution was measured for a series of rotational speeds. The heat generation is due to the torque developed. Here two types of torques were considered, one is the load torque and other is the viscous torque. The heat generation value was inputted with the required conditions and the temperature profile; total heat flux of the entire model was measured. The obtained temperature from the thermal analysis was inputted by updating the conditions. The deformation of the model and the maximum stress distribution at the contact were measured. At higher speeds the dynamic response was significant and the thermal effects have to be considered. The thermal load affects the stiffness. The heat generation in the ball bearing is a major cause of thermal expansion

S. No	Rotational Speed (RPM)	Temperature (K)	
		Inner Ring	Outer Ring
1	1000	415	412
2	1100	436	433
3	1200	454	449
4	1300	470	465
5	1400	488	482
6	1500	507	502

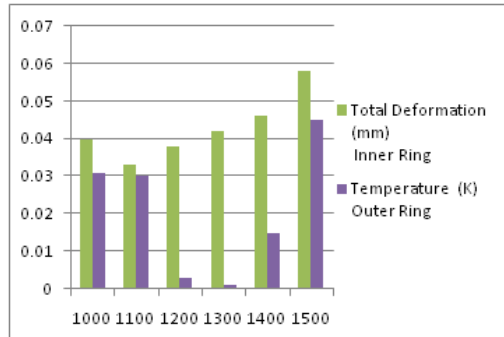


Figure 15. Rotational Speed Vs Temperature

S.No	Rotational Speed (RPM)	Total Heat Flux (W/mm ²)	
		Inner Ring	Outer Ring
1	1000	0.019	0.0022
2	1100	0.023	0.0026
3	1200	0.025	0.0031
4	1300	0.031	0.0035
5	1400	0.034	0.0038
6	1500	0.035	0.0039

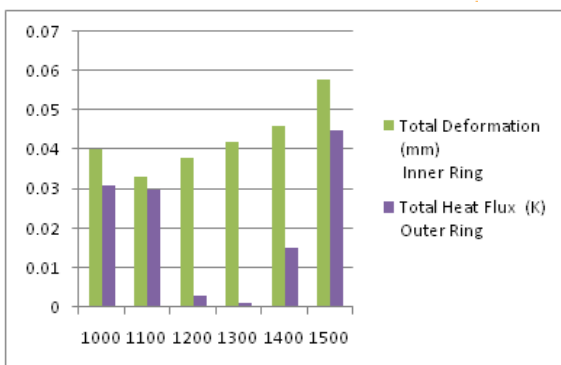


Figure 16. Rotational Speed Vs Total heat flux

S. No	Rotational Speed (RPM)	Equivalent Stress (H bar)	
		Inner Ring	Outer Ring
1	1000	77.84	9.46
2	1100	26.64	3.23
3	1200	33.21	4.53
4	1300	36.76	5.01
5	1400	45.30	5.50
6	1500	98.3	13.44

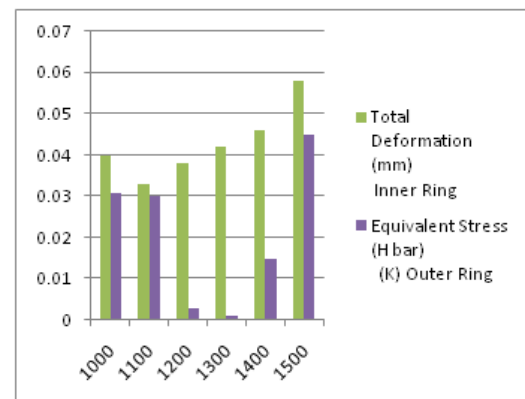


Figure 17. Rotational Speed Vs Equivalent Stress

S.No	Rotational Speed (RPM)	Equivalent Elastic Strain (mm/mm)	
		Inner Ring	Outer Ring
1	1000	0.003	0.0005
2	1100	0.004	0.0007
3	1200	0.005	0.0008
4	1300	0.006	0.0016
5	1400	0.007	0.0014
6	1500	0.010	0.0015

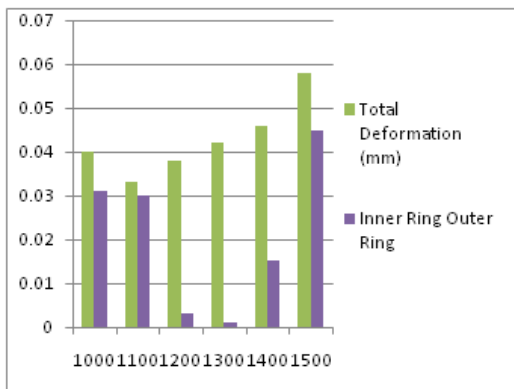


Figure 18. Rotational Speed Vs Equivalent Elastic Strain

S. No	Rotational Speed (RPM)	Total Deformation (mm)	
		Inner Ring	Outer Ring
1	1000	0.04	0.031
2	1100	0.033	0.03
3	1200	0.038	0.003
4	1300	0.042	0.001
5	1400	0.046	0.015
6	1500	0.058	0.045

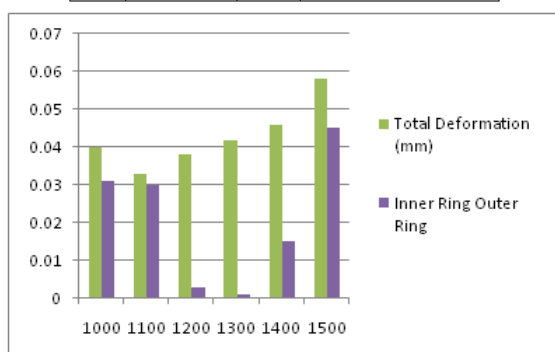


Figure 19 .Rotational Speed Vs Total Deformation (mm)

Conclusion:

The heat generation rate, temperature profile, deformation and thermal stress of the bearing were measured. The simulation was performed, and the temperature increases with heat generation. The effects of temperature for different bearing speeds are studied and the rotational speeds have major effect on the temperature which tends to increase with the increase of speeds. If the groove diameter is reduced, deformation and stresses can be minimized. From the results, deformation is within the limit. This study is used to analyze the failure of bearing.

5. References:

1. Anbazhagan AMS, Anand MD. Design and crack analysis of pressure vessel saddles using finite element method. Indian Journal of Science and Technology. 2016 Jun; 9(21):1- 12.
2. Krishnamani S, Mohanraj T. Thermal analysis of ceramic coated aluminum alloy piston using finite element method. Indian Journal of Science and Technology. 2016 Jun; 9(22):1-5.
3. Alfares MA, Abdallah, Elsharkawy A. Effects of axial preloading of angular Contact ball bearings on the dynamics of a grinding machine spindle system. Journal of Materials Processing Technology. 2003; 136:48-59.
4. Jedrzejewski J, Kwasny W. Modeling of angular contact ball bearings and axial displacements for high-speed spindles. Manufacturing Technology. 2010; 59:377-82.
5. Bao-min W, Xue-Song M, Chi-bing H. Effect of inner ring centrifugal displacement on the dynamic characteristics of high-speed angular contact ball bearing. International Conference on Mechatronics and Automation; 2010.



6. Gao J, Zhang R. Contact simulation of thrust ball bearing based on ANSYS. *Advanced Materials Research*. 2010; 154–155:1629–33.
7. Jin C, Wu B, Hu Y. Heat generation modelling of ball bearing based on internal load distribution. *Tribology International*. 2011.
8. Guo B, Han YQ, Lei WJ. Finite element analysis of hybrid ceramic ball bearing contact. *Key Engineering Materials*. 2011; 474–476:2064–70.
9. Wang C, Yul W, Ren C. An accurate method for calculating the contact subsurface Stress field of hybrid ceramic ball bearing. *Solid State Phenomena*. 2011; 175:215–18
10. Yu DM, Shangb CP, Wang D, Gao ZH. Bearing loads study for high-speed motorized spindle. *Key Engineering Materials*. 2011; 480–481:1511–15.
11. Yin B, Xia X. Key technology of contact problem of deep groove ball bearing based on ANSYS. *Advanced Materials Research*. 2011; 230–232:1067–71.